2022

Preliminary Results of Magnetic and Temperature Map System for 3 GHz Superconducting Radio Frequency Cavities

Ishwari Parajuli
Old Dominion University, ipara001@odu.edu

Bashu Khanal
Old Dominion University, bkhan001@odu.edu

Gianluigi Ciovati
Old Dominion University, gciovati@odu.edu

Jean Delayen
Old Dominion University, jdelayen@odu.edu

Alex Gurevich
Old Dominion University, agurevic@odu.edu

Original Publication Citation

Parajuli, I., Khanal, B., Ciovati, G., Delayen, J., & Gurevich, A. (2022). Preliminary results of magnetic and temperature map system for 3 GHz superconducting radio frequency cavities. In F. Zimmermann, H. Tanaka, P. Sudmuang, P. Klysuban, P. Sunwong, T. Chanwattana, C. Petit-Jean-Genaz, & V.R.W. Schaa (Eds.), *Proceedings of the 13th International Particle Accelerator Conference* (pp. 1315-1318). Joint Accelerator Conferences Website. http://dx.doi.org/10.18429/JACoW-IPAC2022-TUPOTK044

ISBN: 978-3-95450-227-1 ISSN: 2673-5490 doi:10.18429/JACoW-IPAC2022-TUPOTK044

PRELIMINARY RESULTS OF MAGNETIC AND TEMPERATURE MAP SYSTEM FOR 3 GHz SUPERCONDUCTING RADIO FREQUENCY CAVITIES*

I. Parajuli†, B. Khanal, G. Ciovati[1], J. Delayen and A. Gurevich, Old Dominion University, Norfolk, USA
[1]also at Jefferson Lab, Newport News, USA

Abstract

Superconducting radio frequency (SRF) cavities are fundamental building blocks of modern particle accelerators. When we cool these cavities at cryogenic temperature ~2 – 4 K, we can get optimum performance by minimizing RF losses on the inner cavity surface. However, temperature-independent residual losses in SRF cavities cannot be prevented entirely. One of the leading sources of residual losses in SRF cavities is trapped magnetic flux. The flux trapping mechanism depends on different surface preparations and cool-down conditions. We have designed, developed, and commissioned a combined magnetic (B) and temperature (T) mapping system using anisotropic magneto-resistance (AMR) sensors and carbon resistors to study the flux trap mechanism in 3 GHz single-cell niobium cavities. In this contribution, we present the preliminary results of the newly commissioned B & T mapping system.

INTRODUCTION

Niobium (Nb) is an elemental superconductor used to fabricate cavities, the fundamental building block of modern particle accelerators. Superconducting radio frequency (SRF) cavities are resonators, which can be excited by the rf field to get the maximum electric field along their axis. SRF cavities operate at cryogenic temperatures 2-4 K to reduce the temperature-dependent, BCS surface resistance. However, the temperature-independent residual resistance provides a lower limit to the quality factor, Q_0, of the SRF cavities. There are several contributors to the residual losses [1, 2], a major one being the magnetic flux trapped on the cavity surface. To understand the mechanism of trapped flux on the cavity surface, diagnostic tools are in high demand.

We have designed, developed, and commissioned a combined magnetic and temperature map (B&T map) system using anisotropic magneto-resistance sensors (AMR) and carbon resistors to study the flux trap mechanism in 3 GHz single-cell niobium cavities. This contribution presents the preliminary results of the newly commissioned B & T mapping system.

* Work supported by NSF Grant 100614-010. Jlab work is supported by Jefferson Science Associates, LLC under U.S. DOE Contract No. DE-AC05-06OR23177.
† ipara001@odu.edu

EXPERIMENTAL SETUP AND PROCEDURE

Thermometry System

The temperature map system was designed based on the system originally developed at Cornell University for 1.5 GHz cavities [3] and adopted at Jefferson Lab for 1.3 GHz and 1.5 GHz cavities [3, 4]. There are 88 Allen-Bradley carbon resistors (100 Ω) in the T-map system, which are used as resistance-temperature devices (RTD). Their sensitivity is ~10 Ω/mK at 2 K. Details about the fabrication of the thermometer can be found in [3, 4]. Eight printed circuit boards (PCB) of G10 material are designed and machined to place the 11 thermometers in contact with the cavity surface. Figure 1 shows a picture of a thermometer board. The spacing between each thermometer is ~1 mm. The thermometers were excited by ~5 μA current at 2 K so that the typical voltage drop across 7 kΩ resistors is ~35 mV.

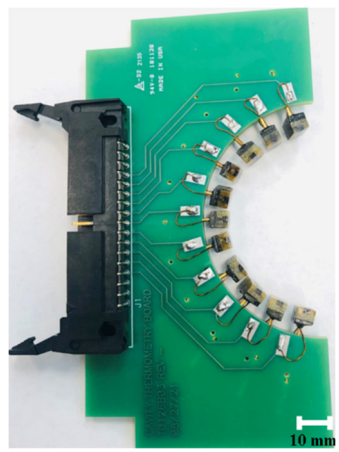

Figure 1: Complete thermometry board.

The SCXITM system from National Instrument was used to measure the voltage across 88 thermometers. Four SCXI-1102 modules are connected to a single SCXI-1001 chassis. Each SCXI-1102 module is capable of multiplexing 32 differential inputs. A Keithley 2400 source meter was used to provide the excitation voltage to the thermometers. The helium bath temperature was measured as the average of the temperature measured with four calibrated Cernox sensors and a Lakeshore 218 temperature monitor.

Magnetometry System

Figure 2 shows the schematic diagram of a magnetic field sensor assembly. It consists of two AMR sensors [5-

ISBN: 978-3-95450-227-1 ISSN: 2673-5490 doi:10.18429/JACoW-IPAC2022-TUPOTK044

11]: AMRt and AMRr. AMRt measures the tangential component of the magnetic field on the cavity surface whereas AMRr measures the radial component of the magnetic field. The AMR sensors were calibrated at liquid He temperature in a separate setup. A total of 40 magnetic field sensor assemblies were used, each with 2 AMR sensors. Eight printed circuit boards (PCB) of G10 material are designed and machined to place 5 B-sensors in contact with the cavity surface. The spacing between each sensor is ~12 mm. Figure 3 shows a picture of a board with five B-sensors.

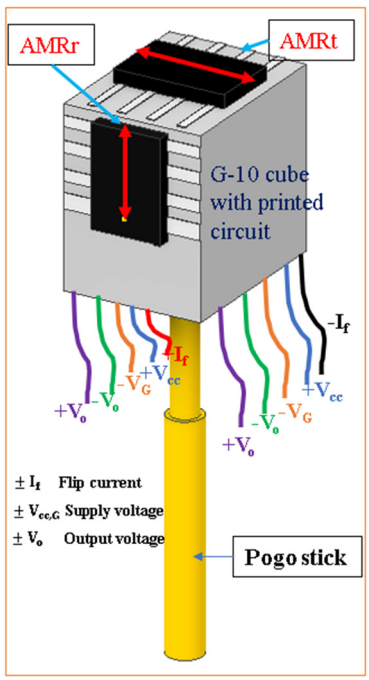

Figure 2: Schematic diagram of B-sensor.

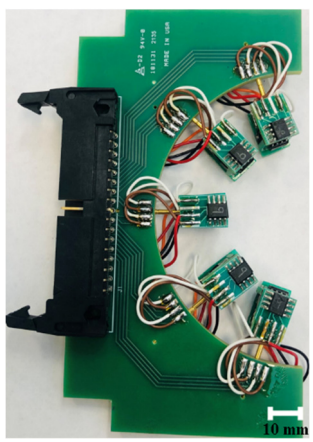

Figure 3: Complete B-sensor board.

The PXIe system from National Instrument was used to measure the voltage from AMR sensors. Four PXIe-4302 modules were connected to a PXIe-1075 chassis. A PXIe-8360 controller was connected to the PXIe-1075 chassis. Data were acquired with a computer with a PCIe-8361 remote controller card. A pulsed current source (model 2611, Keithley Instruments, USA) is used to drive the flip coil of the AMR sensors, and a power supply was used to provide a supply voltage of 9 V to the sensors. The instrument control and data acquisition were performed using programs written in LabVIEW™.

Electrical Connection and Final Assembly

Four half-ring aluminum plates are attached to the bottom and top beam tubes of the cavity. Each ring contains 16 radial grooves with 22.5° angular spacing, into which thermometry and B-sensor assembly boards are alternated. Figure 4 shows the B-sensor and thermometry boards being inserted in the grooves of the rings. Sixteen twisted-pair flat ribbon cables connect the sensor boards to a feedthrough box mounted on the test stand top plate. The signals were routed from the feedthrough box to the data acquisition system using sixteen shielded jacketed ribbon cables.

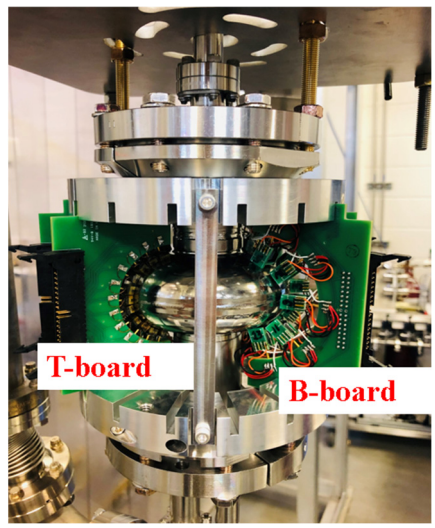

Figure 4: Thermometry and B-sensors board assembled to the cavity.

Experimental Procedure

The experimental procedure was as follows:

- The 3 GHz large grain Nb cavity labeled “FH3F” [12] was high-pressure rinsed with ultra-pure water and assembled in the cleanroom. The cavity was evacuated on a vertical test stand and the B & T system was assembled onto the cavity, outside the cleanroom.
- The test stand was inserted in a Dewar at JLab’s Vertical Test Area. The residual magnetic field at the cavity location was ~3 mG. A current pulse of 300 µs width and 150 mA amplitude was applied to the B-sensors to reset their magnetization. After that, the cavity was cooled to ~10 K > T_c. We measured the B-sensors’ offset voltages in a low residual DC magnetic field, B_a ~3 mG.
- B_a was varied by changing the current in the compensation coils wound around the Dewar and then we performed cool-down to 4.3 K with either ΔT ~ 5 K along the cavity axis (“fast” cool-down) or ΔT ~ 0.15 K along the cavity axis (“slow” cool-down). Once cool-down was done B_a was lowered to ~3 mG.

ISBN: 978-3-95450-227-1 ISSN: 2673-5490 doi:10.18429/JACoW-IPAC2022-TUPOTK044

- Once the cavity is immersed in liquid helium (4.2 K), the He bath pressure was lowered to 23.5 Torr, corresponding to a temperature of 2 K. The RTDs calibration was done between 4.2 K to 2 K. At the same time, $Q_0(T)$ was measured at a low RF field.
- $Q_0(E_{acc})$ was measured at 2 K along with B &T maps.

RESULTS

Figure 5 shows the quality factor versus accelerating gradient measured with different cool-down conditions in different magnetic fields. In all tests, the cavity performance was limited due to quenching at ~19 MV/m, corresponding to a peak surface magnetic field of 80.4 mT. There was no detectable field emission in any of the RF tests.

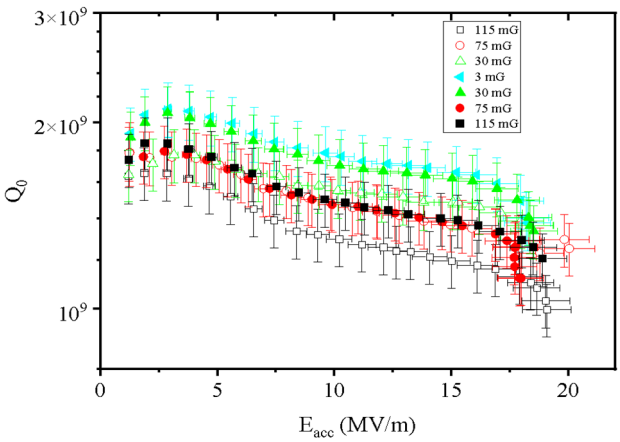

Figure 5: Quality factor versus accelerating gradient measured at 2 K after fast cool-down (solid symbols) and after slow cool-down (empty symbols).

Figure 6 shows the residual resistance versus the applied magnetic field.

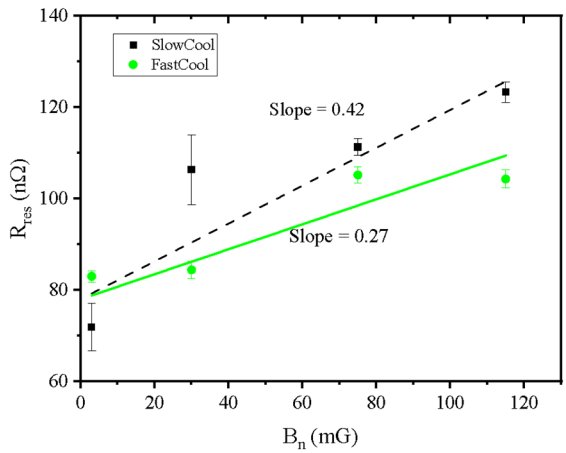

Figure 6: Residual resistance measured after fast cool-down at the different ambient magnetic fields (circles) and after slow cool-down at the different ambient magnetic fields (squares). Solid and dashed lines are weighted linear fits of the corresponding data.

Following Eqs. (2) and (3) of Ref. [13], the flux trap sensitivity was found to be 0.42 nΩ/mG, and the trapping efficiency was found to be 64%.

Figure 7(a) shows, as an example, the temperature distribution on the cavity surface recorded by the T-maps at 18 MV/m, just before the quench. Figure 7(b) shows the quench location (270°-3rd) detected by T-map during the quench. Both T-maps were taken during the RF test after a slow cool-down at ~115 mG. B-maps taken during quench after slow cool-down at ~30 mG and ~115 mG are shown in Figs. 8 (a) and (b), respectively.

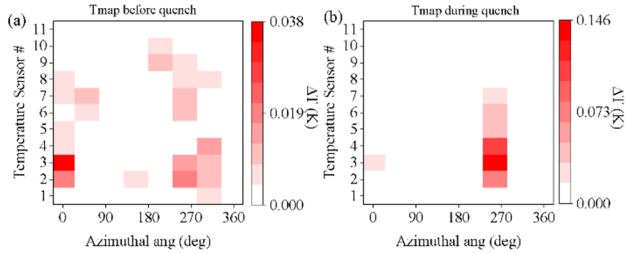

Figure 7: T-map just before quench (a) and during quench (b).

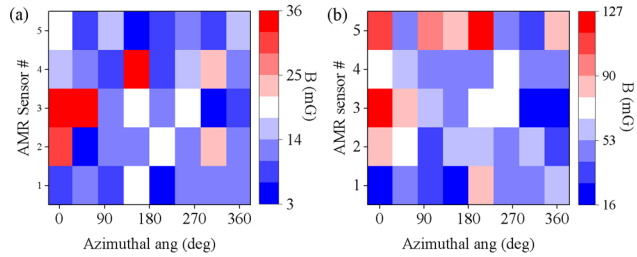

Figure 8: B-map during quench after slow cooldown with ~30 mG (a) and ~115 mG (b). Notice the difference in the B-scale.

CONCLUSION

We have designed, developed, and commissioned a new B&T mapping system for 3 GHz cavities. The first result of the newly commissioned system showed that the T-map system is capable of detecting hot spots and quench locations on the surface of the 3 GHz SRF cavity. Different distribution of trapped flux was measured after different cool-down and residual B-field, however, no variation in magnetic field distribution was observed during the quench, likely due to magnetic sensors being far from the quench location.

ACKNOWLEDGMENTS

We would like to acknowledge JLab SRF staff members for their technical and cryogenic support.

REFERENCES

[1] H. Padamsee, J. Knobloch, and T. Hays, *RF Superconductivity for Accelerators,* Wiley & Sons, New York, 1998.

[2] A. Romanenko, A. Grassellino, O. Melnychuk, and D.A. Sergatskov. "Dependence of the residual surface resistance of superconducting radio frequency cavities on the cooling dynamics around Tc", *J. Appl. Phys.,* vol. 115, p.184903, 2014.

[3] J. Knobloch, Ph.D. Thesis, Cornell University, 1997.

[4] G. Ciovati *et al.*, "Temperature mapping system for single-cell cavities", JLAB-TN-05-059, 2005.

ISBN: 978-3-95450-227-1 ISSN: 2673-5490 doi:10.18429/JACoW-IPAC2022-TUPOTK044

[5] I.P. Parajuli, G. Ciovati, J.R. Delayen, and A.V. Gurevich, "Evaluation of Anisotropic Magnetoresistive (AMR) Sensors for a Magnetic Field Scanning System for SRF Cavities", *in Proc. IPAC'21*, Campinas, SP, Brazil, May 2021, pp. 2304-2307. doi:10.18429/JACoW-IPAC2021-TUPAB344.

[6] I.P. Parajuli, G. Ciovati,,and J.R. Delayen. "Magnetic field sensors for detection of trapped flux in superconducting radio frequency cavities", *Rev. Sci. Instrum.,* vol. 92, no. 10, p. 104705, 2021.

[7] T. Okada, E. Kako, T. Konomi, M. Masuzawa., H. Sakai, K. Tsuchiya, and T. Tajima, "Systematic evaluation of magnetic sensitivities of anisotropic magnetoresistive sensors at liquid helium temperature for superconducting cavities", *Rev. Sci. Instrum.,* vol. 92, no. 3, p. 035003, 2021.

[8] R. Ueki *et al.*, "Study on magneto-resistance sensors for low magnetic field measurements", *IEEE Trans. Appl. Superconduc.,* vol. 30, no 4, pp. 1-4, 2020.

[9] B. Schmitz, J. Köszegi, K. Alomari, O. Kugeler, and J. Knobloch. "Magnetometric mapping of superconducting RF cavities", *Rev. Sci. Instrum.,* vol. 89, no. 5, p. 054706, 2018.

[10] T. Okada *et al.*, "Development of Temperature and Magnetic Field Mapping System for Superconducting Cavities at KEK", *in Proc. SRF'19*, Dresden, Germany, Jun.-Jul. 2019, pp. 583-585. doi:10.18429/JACoW-SRF2019-TUP060.

[11] S.N. Lobo, M. Liepe, and T.E. Oseroff, "Magnetic Field Mapping System for Cornell Sample Host Cavity", *in Proc. SRF'19*, Dresden, Germany, Jun.-Jul. 2019, pp. 961-963. doi:10.18429/JACoW-SRF2019-THP046.

[12] G. Ciovati, G. Eremeev, and F. Hannon. "High field Q slope and the effect of low-temperature baking at 3 GHz", *Phys. Rev. Accel. Beams*, vol. 21, no. 1, p. 012002, 2018.

[13] P. Dhakal, G. Ciovati, and A. Gurevich. "Flux expulsion in niobium superconducting radio-frequency cavities of different purity and essential contributions to the flux sensitivity", *Phys. Rev. Accel. Beams,* vol. 23, no. 2, p. 023102, 2020.